Idle sense with transmission priority in fibre-wireless networks

IET Communications

Research Article

IET Journals
The Institution of Engineering and Technology

Idle sense with transmission priority in fibre-wireless networks

ISSN 1751-8628
Received on 11th April 2019
Revised 10th October 2019
Accepted on 29th January 2020
E-First on 8th April 2020
doi: 10.1049/iet-com.2019.0313
www.ietdl.org

Wan Hafiza Wan Hassan[1,2] ✉, Sevia Mahdaliza Idrus[2], Horace King[3], Shabbir Ahmed[3], Mike Faulkner[3]

[1]*Faculty of Ocean Engineering Technology and Informatics, Universiti Malaysia Terengganu, Terengganu, Malaysia*
[2]*Faculty of Engineering, Universiti Teknologi Malaysia, Johor, Malaysia*
[3]*College of Engineering and Science, Victoria University, Melbourne, Australia*
✉ *E-mail: whafiza@umt.edu.my*

Abstract: The convergence of fibre and wireless technologies realised the fibre-wireless (FiWi) networks. Despite huge capacity offered by fibre, the user experiences a network bottleneck caused by the wireless side. This study investigates wireless local area network (WLAN), the wireless side of the FiWi networks with a gigabits passive optical network (GPON) as the backhaul. The work aims to improve WLAN performance by utilising information gained from GPON. The proposed technique enables all contending stations in multiple access points (APs) WLAN to achieve a desired downlink-to-uplink transmission ratio, k while maintaining maximum throughput. Optimum contention window (CW) sizes for the APs and associate wireless users (WUs) are derived by incorporating the principles of idle sense (IS) and asymmetric AP. However, fairness problem between WUs occurred when they contend the channel with different CW sizes. Hence, this study simplifies the IS scheme to increase fairness between WUs. Furthermore, AP self-adapting and WU adjusting algorithms are proposed to assist the network to achieve the desired *k*, while maintaining the throughput fairness amongst basis service sets. The robustness of the proposed scheme is demonstrated under various conditions: achieved target *k* with nearly perfect fairness and gained near-to-maximum throughput within 96% of the theoretical optimum.

Nomenclature

p_{ap}	probability of an AP transmitting
p_{wu}	probability of a WU transmitting
m	total number of APs (or BSSs)
n	total number of WUs
CW_{ap}	current contention window size for an AP
CW_{wu}	current contention window size for a WU
P_s^{ap}	probability that a transmission is a successful AP transmission
P_s^{wu}	probability that a transmission is a successful WU transmission

1 Introduction

Fibre-wireless (FiWi) networks have evolved as a promising broadband access network as it offers a huge capacity of bandwidth from the fibre and freedom of mobility from the wireless side [1–6]. The survey conducted in [7] found that the European broadband subscriber valuation of fibre to the home (FTTH) connection has increased quickly over time and became significantly higher than the valuation of digital subscriber line at the end of the survey in December 2014. Furthermore, the number of FTTH subscribers in Europe increased by 20.4% since September 2016 with more than 51.6 million FTTH subscribers in September 2017 [8]. This FTTH termination is likely to use wireless distribution throughout the home.

A passive optical network (PON) is adopted as the backhaul for FiWi networks due to its energy efficiency and reliable service provision. The PON in this network acts as a small cell backhaul, a promising solution to satisfy the ever increasing demand for mobile data traffic [9–12]. Previous work in [9] showed a small cell backhaul deployment using PON can halve the cost in comparison with the typical point to point fibre backhauling approach. On the wireless side, the work in [10, 11] proposed wireless mesh networks to provide network survivability and the work in [12] opted to integrate with the WiFi function in small cell backhaul to avoid the huge data loss and traffic outage when a distribution fibre is broken. Similarly, the work in [13] proposed FiWi networks by integrating gigabits passive optical network (GPON) as a small cell backhaul with a 'closed' infrastructure wireless local area network (WLAN) in the wireless side, as shown in Fig. 1.

The optical line terminal (OLT) of GPON at the central office is connected to a passive optical splitter, which divides the optical power into *m* separate paths to the subscribed optical network terminals (ONTs). Each ONT in FiWi networks is directly connected to the AP of the WLAN. In this situation, the operator has a dedicated spectrum allocation, which is shared by all access points (APs). Such a scenario may result in massive traffic congestion if the APs are closely located (adjacent properties or apartment), which is often the case for GPONs in dense urban and sub-urban areas. The congestion gets worse when each AP has an increasing number of associated wireless users (WUs). Hence, this study focuses on the techniques to improve the quality of service (QoS) of the densely deployed WLAN pertaining to the fairness among the transmitting terminals by exploiting the information gained from the GPON side.

In this study, WLAN, using the idle sense (IS)-based medium access control (MAC) method, is chosen as the front end for FiWi integration due to its simplicity, low cost of implementation and its ability to operate in either dedicated or unlicensed spectrum.

In practice, the majority of WLAN deployments operate in an infrastructure mode that comprises an AP serving its associate WUs forming a basic service set (BSS). The same deployment is applied to the front end of the proposed FiWi networks as shown in Fig. 1. In return, the AP in each BSS is the gateway for all the WUs, which requires more transmission opportunities than each WU. However, in the standard IEEE 802.11 distributed coordination function (DCF) access method, every station including the AP is given an equal chance of transmission, which leads to unfairness between uplink (UL) and downlink (DL) transmissions, thus, degrading the QoS in WLAN.

Extensive works have been carried out to mitigate the UL and DL unfairness [14–25]. In common, the schemes propose priority access for the AP. The authors in [18–20, 24] change the CW_{min} of the contending stations in accordance with the target DL/UL ratio.

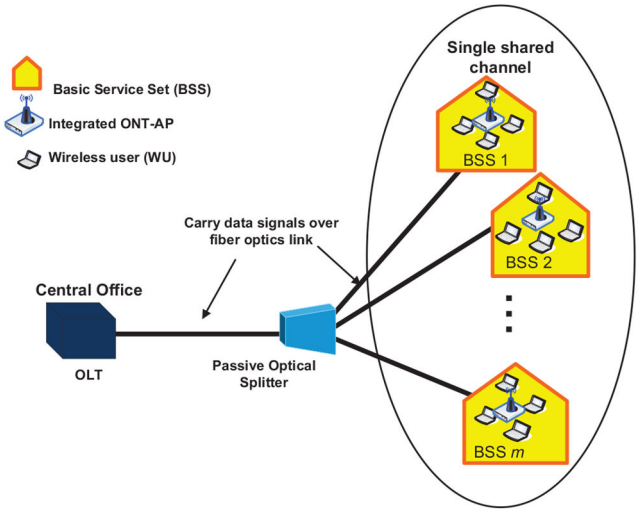

Fig. 1 *Proposed FiWi networks [13]*

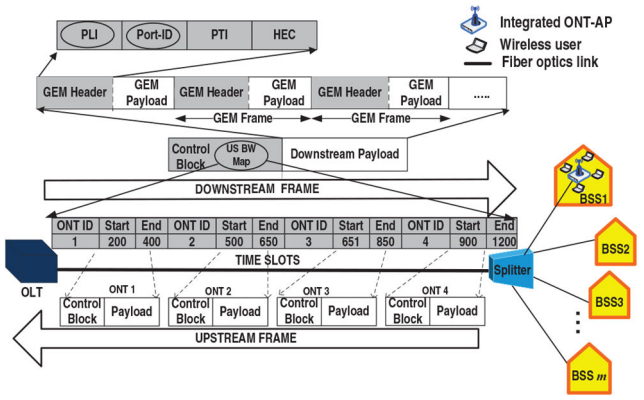

Fig. 2 *GPON frame format [13, 31]. Shaded frames are non-encrypted and can be accessed by all ONTs. Circled subfields are used as potential estimates*

Furthermore, the methods proposed in [22, 23] reduce inter frame spacings (PIFS and SIFS instead of DIFS) of the AP while authors in [24, 25] adjust the transmission opportunity limits of the AP. On the contrary, Umehara *et al*. [17] proposed a DCF with successful transmission priority only for the UL transmission with the assumption that the AP does not have any data flow to WUs. The scheme provides the success of WUs higher priority by using a variety of IFS including SIFS and PIFS. Recently, Katayama *et al*. [15] proposed the same approach to adjust the back-off time at the AP in order to allocate more DL bandwidth in high-density WLAN.

Alternatively, Ando *et al*. [16] used a unique synchronised phase (SP) with phase shifting to set the back-off time rather than using a random integer in CSMA/CA. A new amplitude parameter is introduced in the SP technique to allow (the AP to get higher transmission opportunities than WUs. Among all, the asymmetric AP (AAP) scheme proposed in [21] is seemed to be promising due to its efficiency and simplicity. It scales the CW size of an AP and allows the WUs to use the IS method [26] as their CW adaptation mechanism.

However, AAP and all other priority schemes discussed above have been proposed for QoS enhancement and to provide DL/UL fairness in a single BSS infrastructure network. They are less suitable for an infrastructure WLAN where there are multiple APs sharing the same spectrum and each serving its own BSS of associated WUs. Little attention has been paid to the multiple AP scenarios despite the fact that this network scenario represents the wireless side of FiWi networks that are becoming increasingly popular [1–6]. Hence, this study focuses on the fairness problem of multiple APs sharing the same spectrum scenarios in the FiWi networks (Fig. 1). We extend the throughput analysis in the AAP scheme [21] to the multiple AP scenario and derived the optimum CW size of the APs.

On the other hand, the IS technique used in the AAP scheme allows every WU to dynamically control its CW size by monitoring the mean number of idle slots between transmission attempts. It is a simple method using a local estimate without involving an intermediate state of estimating the number of stations, which is difficult to obtain accurately and may cause instability to the system [27]. IS is claimed in [28] as one of the arguably best time fairness-based channel access algorithms. However, it is noteworthy that the previous authors involved in the IS scheme assumed all stations have similar CW sizes [21, 26, 29, 30]. This assumption is not always valid in a real deployment of WLAN because of local interference factors. Therefore, we initiate WU with different CW sizes as a means to test the robustness of the scheme. We show that when the number of APs increases the fairness between WUs deteriorate, caused by the adjustment algorithm in IS. To overcome the problem, we propose an alternative way of achieving the desired UL/DL ratio, fairness, and maximum throughput.

All the techniques proposed in this work do not require information about any unknown variable except for the number of APs, m. However, the value of unknown m can be estimated by exploiting information from the GPON. Thus, the following section describes the GPON frame structure. The remaining sections of the paper are organised as follows: Section 3 extends the principles of AAP and IS methods in multiple APs scenario and derives the optimum AP and WU contention window (CW) sizes. Section 4 describes the simulation set up in this work. Section 5 evaluates the performance of IS with transmission priority technique in multiple BSSs environment. Section 6 presents synchronous updates to reduce the fairness problem in the proposed scheme. Sections 7 and 8 propose an AP self-adapting (APSA) and a WU adjustment (WUA) algorithms, respectively, to further improve the fairness of the scheme. Finally, Section 9 concludes the paper.

2 GPON frame structure

This section describes how the estimate for m (number of APs) is established by exploiting the existing standardised technologies of GPON. Fig. 2 illustrates the GPON upstream and downstream frames as specified in [31]. The broadcast nature of downstream transmissions allows ONTs to retrieve network traffic information. The downstream payload comprises a series of GPON encapsulation method frames, which consists of a header and an encrypted payload. First, the contents of the Port-ID and payload length subfields contain the information of the owner of the payload and the corresponding payload size, respectively. This provides an estimate on the number of active ONTs and the size of the down-stream traffic going into the ONTs, which in turn is the total traffic transmitted from APs to WUs. Second, the upstream bandwidth mapping (US BW Map) subfield within the downstream control block broadcast the schedules for the selected ONTs to transmit upstream. Each selected ONT is granted an amount of time to transmit in accordance with the traffic information of each ONT buffer passed over the upstream control block subframe to the OLT. Analysing the US BW Map subfield provides another estimate for the total number of active ONts and the total size of upstream traffic. Hence, the total number of active integrated APs at the air interface can be estimated by combining the estimate of active ONTs on the upstream and the downstream lines through the extraction of information from the Port-ID and the US BW Map subfields, respectively.

For simplification, two assumptions are made in this work. First, all the GPON traffic goes directly to the WLAN and the WLAN channel is only dedicated to the GPON traffic. As such, each ONT from the splitter is directly connected to the corresponding AP in the WLAN. Second, a perfect transmission is assumed from the OLT to each ONT with the extracted GPON traffic information made available in the AP of each BSS through the networks integration process as illustrated in Fig. 3.

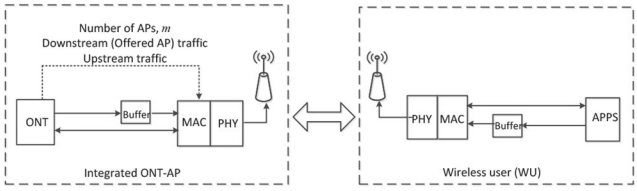

Fig. 3 *Proposed FiWi network scenario with traffic indicators*

The integration is employed at the end-user terminal where an ONT of GPON and an AP of WLAN are incorporated into a single device, forming a FiWi hybrid system (also known as radio and fibre system) [1–3, 5]. The integrated ONT–AP device acts as a gateway translating MAC frames from the optical network to the wireless network and vice versa. Two distinct separate MAC protocols are used to access GPON and WLAN, respectively. Thus, the wireless MAC frames only traverse the WLAN and do not have to travel along the optical fibre to be processed at the central office, avoid the negative impact of the fibre propagation delay on the network [5, 32]. Considering the fact that separate MAC protocols are used, the scope of this study is fully focusing on the WLAN side performance by using the information gained from the GPON to estimate m. The following section will present how the estimate m is utilised to improve WLAN performance.

3 Transmission priority in multiple APs scenario

This section analytically derives optimum CW sizes for an AP and a WU in the WLAN network. Our proposed network scenario resembles the wireless side of the FiWi network architecture. It comprises m-integrated ONT-APs and n-associated WUs, where each AP serves its own BSS of n/m-associated WUs. The worst case scenario in terms of frequency availability in densely populated urban areas is considered. All BSSs are within close proximity, i.e. all wireless stations, APs and WUs, share one single channel and can hear each other, albeit being potential interferers. The spectrum is considered 'closed', i.e. a single 20 MHz channel entirely dedicated to this network. This assumption is inline with the concept of the small cell backhaul in FiWi networks as proposed in [9, 10, 12]. It is also assumed that all stations always have packets to transmit (i.e. greedy stations) and are given an infinite number of trials until the packet is successfully transmitted.

The following analysis is carried out by combining the principles of AAP [21] and IS [26, 29]. The aim is to give the APs the priorities to have the required bandwidth, which is $1/k$ time bigger than the WUs. Thus, the remaining bandwidth is shared by all WUs in a fair manner. Now, consider m APs and n WUs are contending the WLAN channel with CW sizes of $\mathrm{CW_{ap}}$ and $\mathrm{CW_{wu}}$, respectively, the probability that there is at least one transmission is given by

$$P_{\mathrm{tr}} = 1 - (1 - p_{\mathrm{ap}})^m (1 - p_{\mathrm{wu}})^n \tag{1}$$

where p_{ap} and p_{wu} are the probability of an AP and a WU transmitting, respectively. See Nomenclature section for a list of notations. The probabilities p_{ap} and p_{wu} are independent of each other and are given by the following based on Bianchi's model in [33]

$$p_{\mathrm{ap}} = \frac{2}{(\mathrm{CW_{ap}} + 1)} \tag{2}$$

and

$$p_{\mathrm{wu}} = \frac{2}{(\mathrm{CW_{wu}} + 1)}. \tag{3}$$

Furthermore, the probability that a transmission is a successful AP transmission $P_{\mathrm{s}}^{\mathrm{ap}}$ is given by the probability that only one AP transmits on the channel provided that there is a transmission

$$P_{\mathrm{s}}^{\mathrm{ap}} = \frac{m p_{\mathrm{ap}} (1 - p_{\mathrm{ap}})^{m-1} (1 - p_{\mathrm{wu}})^n}{P_{\mathrm{tr}}}. \tag{4}$$

Similarly, the probability that a transmission is a successful WU transmission is given by

$$P_{\mathrm{s}}^{\mathrm{wu}} = \frac{n p_{\mathrm{wu}} (1 - p_{\mathrm{ap}})^m (1 - p_{\mathrm{wu}})^{n-1}}{P_{\mathrm{tr}}}. \tag{5}$$

A transmission priority factor k can now be introduced. It is defined as the number of successful transmissions of APs with respect to WUs

$$k = \frac{P_{\mathrm{s}}^{\mathrm{ap}}}{P_{\mathrm{s}}^{\mathrm{wu}}} = \frac{n p_{\mathrm{wu}} (1 - p_{\mathrm{ap}})}{m p_{\mathrm{ap}} (1 - p_{\mathrm{wu}})}. \tag{6}$$

A value of $k > 1$ implies higher DL throughput; while a value of $k < 1$ represents higher UL throughput. In this study, the value of k is set globally in accordance with the network demand.

Rearrange (6) with approximation $(p_{\mathrm{wu}}/1 - p_{\mathrm{wu}}) \simeq p_{\mathrm{wu}}$, at which p_{wu} is always relatively small ($p_{\mathrm{wu}} \ll 1$), yields

$$\frac{p_{\mathrm{ap}}}{1 - p_{\mathrm{ap}}} = \frac{n p_{\mathrm{wu}}}{km(1 - p_{\mathrm{wu}})} \simeq \frac{n p_{\mathrm{wu}}}{km}. \tag{7}$$

Thus

$$1 - p_{\mathrm{ap}} = \frac{km}{n p_{\mathrm{wu}} + km}. \tag{8}$$

Then, using (8), the probability of an idle slot can be approximated as

$$\begin{aligned} p_i &= (1 - p_{\mathrm{ap}})^m (1 - p_{\mathrm{wu}})^n \\ &\simeq (1 - p_{\mathrm{wu}})^n \left(\frac{km}{n p_{\mathrm{wu}} + km} \right)^m. \end{aligned} \tag{9}$$

According to [21], when all contending stations n use IS with the access probability p, the number of idle slots between two transmissions is kept constant so that the probability of an idle slot p_i also remains constant. Thus, IS maintains $np = \alpha$ with α being some constant and as $n \to \infty$

$$\begin{aligned} p_i^{\mathrm{opt}} &= \lim_{n \to \infty} (1 - p)^n \\ &= \lim_{n \to \infty} \left(1 - \frac{\alpha}{n} \right)^n \\ &\simeq \mathrm{e}^{-\alpha}. \end{aligned} \tag{10}$$

In our scenario, only WUs use IS. The probability of an idle slot remains $p_i^{\mathrm{opt}} \simeq \mathrm{e}^{-\alpha}$, and the access probability of WUs p_{wu} is such that $n p_{\mathrm{wu}} = \beta$, where β is another constant. Then, similar to (10), we thus obtain

$$\begin{aligned} \lim_{n \to \infty} (1 - p_{\mathrm{wu}})^n &= \lim_{n \to \infty} \left(1 - \frac{\beta}{n} \right)^n \\ &\simeq \mathrm{e}^{-\beta}. \end{aligned} \tag{11}$$

Using (10) and (11) in (9) leads to

$$\alpha = \beta - m\ln(km) + m\ln(\beta + km)\,. \tag{12}$$

We can numerically solve (12) to get the value of β as the value of k, m, and α are known. The variable m is estimated from the GPON frame format information as described in Section 2 and the constant α can be obtained by solving $1 - \alpha = (1 - (T_{slot}/T_c))e^{-\alpha}$, a minimised cost function derived in [26]. Then, from (8), we have

$$p_{ap} = \frac{\beta}{\beta + km} \tag{13}$$

and from (2), we have

$$CW_{ap} = \frac{2(\beta + km)}{\beta} - 1. \tag{14}$$

Furthermore, as stated before $np_{wu} = \beta$, then

$$p_{wu} = \frac{\beta}{n}, \tag{15}$$

and from (3), we have

$$CW_{wu} = \frac{2n}{\beta} - 1. \tag{16}$$

All variables in CW size formulations are assumed known and the required MAC and physical layer (PHY) parameters are listed in Table 1.

The derived formulations are validated in terms of saturation throughput. Bianchi's model in [33] is used to analyse the normalised saturation throughput, S. Refer to the Appendix in Section 12 for a full derivation of (17)

$$S = \frac{P_s P_{tr} T_{payload}}{(1 - P_{tr})T_i + P_s P_{tr} T_s + (1 - P_s)P_{tr} T_c}, \tag{17}$$

where $T_{payload}$ is the average time taken to transmit the payload, T_i is the idle slot time defined in the IEEE 802.11 standard [34], T_s is the average time the channel is sensed busy by each station due to a successful transmission, and T_c is the average time the channel is sensed busy by each station due to a collision. The values of T_s and T_c depend on PHY and MAC layers' parameters (defined in IEEE 802.11 standard as listed in Table 1), which can be expressed as

$$T_s = T_{payload} + \text{SIFS} + T_{ACK} + \text{DIFS} \tag{18}$$

and

$$T_c = T_{payload} + \text{DIFS}\,. \tag{19}$$

In addition, the UL throughput S_{wu} and DL throughput S_{ap} are expressed as follows:

$$S_{wu} = \frac{P_s^{wu} P_{tr} T_{payload}}{(1 - P_{tr})T_i + P_s P_{tr} T_s + (1 - P_s)P_{tr} T_c} \tag{20}$$

and

$$S_{ap} = \frac{P_s^{ap} P_{tr} T_{payload}}{(1 - P_{tr})T_i + P_s P_{tr} T_s + (1 - P_s)P_{tr} T_c}\,. \tag{21}$$

The throughputs are computed analytically using (17), (20), and (21), when every station employs a fixed value of CW_{ap}^{opt} and CW_{wu}^{opt} derived in (14) and (16), respectively. All variables in CW size formulations are assumed known in order to obtain the ideal throughputs, known as target throughput. Table 2 presents the optimal CW sizes for APs and WUs as we increase the number of BSSs from 1 to 30 with the transmission priority factor, k, set equal to 1.

Table 1 MAC and PHY parameters based on IEEE 802.11a

Parameter	Value
packet size	8184 bits
MAC header	224 bits
PHY header	20 μs
ACK length	134 bits/control rate + PHY header
data rate	54 Mbps
control rate	6 Mbps
channel bandwidth	20 MHz
slot time	9 μs
SIFS time	16 μs
DIFS time	34 μs
ACK timeout	70 μs

Table 2 CW_{ap}^{opt} and CW_{wu}^{opt} for varying sizes of BSSs

m	n	CW_{ap}	CW_{wu}
1	4	16	57
2	8	30	117
3	12	45	176
4	16	60	236
5	20	75	296
10	40	150	595
15	60	225	894
20	80	299	1193
25	100	374	1492
30	120	449	1791

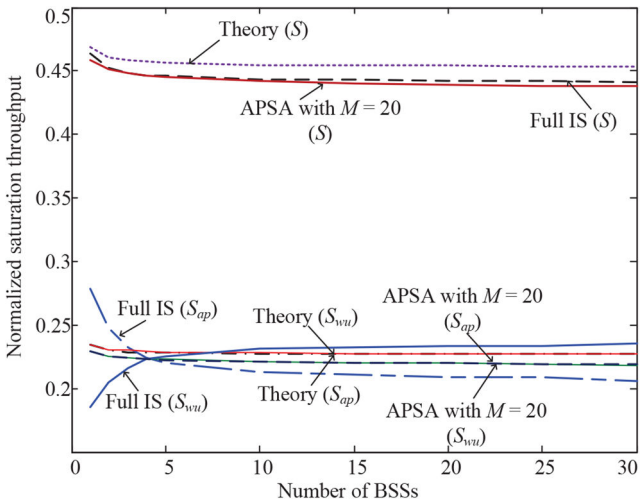

Fig. 4 *Normalised saturation throughput versus m, number of BSSs (simulation and theory)*

The plotted curves (using MATLAB software) in Fig. 4 show the target (theoretical) throughputs (S, S_{wu}, and S_{ap}) when the number of BSSs increases.The curves S_{wu} and S_{ap} are overlaid as expected for $k = 1$.

4 Simulation setup

In this work, the performance of all proposed schemes is evaluated by means of simulation carried out using OPNET Modeler 16.1 software. OPNET is a commercial packet level simulator. It accurately models the behaviour for any kind of network. The WLAN is modelled based on simulation parameters from the IEEE802.11a standard, as listed in Table 1. Every BSS comprises one integrated ONT-AP serving four WUs. Every station is assumed continuously transmitting with a constant packet size of 8184 bits.

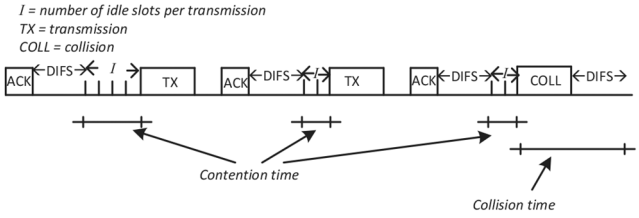

Fig. 5 *Non-productive (wasted) time*

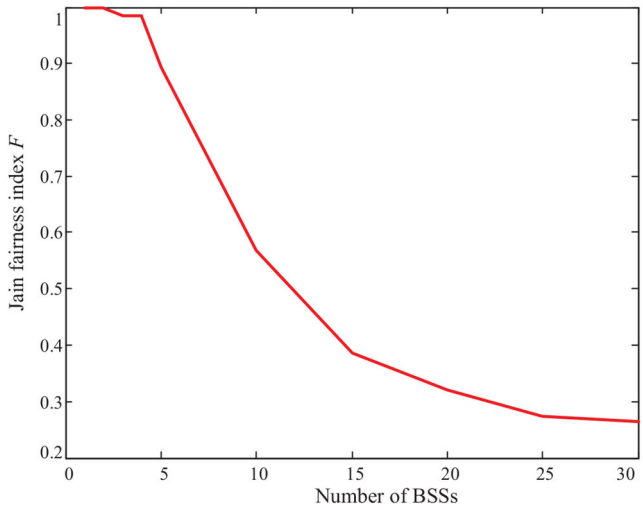

Fig. 6 *Jain fairness index (24) versus m, the number of BSSs. All WUs use full IS while the APs fixed* CW_{ap}^{opt} *as derived in (14)*

5 IS method

In this section, we evaluate the performance of the proposed scheme with the WUs having different initial values of CW_{wu}. The WUs adaptively adjust their CW sizes using the IS algorithm, while the APs fix their CW sizes to CW_{ap}^{opt} as computed in Table 2 and dependent on the number of active interfering BSSs, m, obtained from the GPON header.

IS is developed from the assumption that minimising time spent in the collision state and the contention state will maximise the throughput (Fig. 5). The probability of collision reduces as the contention time increases and vice versa. The optimum trade-off occurs when both times are equal.

The analysis in [26] showed that the optimum number of idle slots per transmission is a function of the number of contending stations, n, but quickly converges to a constant as n goes to infinity. Therefore, in this work, we defined the converged value as the target number of idle slots per transmission, (I_t)

$$I_t = \frac{e^{-\alpha}}{1 - e^{-\alpha}}. \tag{22}$$

The constant α refers to the same constant that has been introduced earlier in (10)–(12). Numerically solved for a value of α (in accordance with MAC and PHY IEEE 802.11a parameters, Table 1) gave us the predefined target value I_t equals to 3.26.

Furthermore, all WUs in IS compare their estimated idle slots per transmission attempt $\hat{I}$ with target value I_t and adapt their CW_{wu} in a distributed manner using the additive increase multiplicative decrease (AIMD) algorithm. The WUs decrease their CW_{wu} by a factor of a 16th when the channel is less busy ($\hat{I} > I_t$) and increase their CW_{wu} by six when the channel is less idle ($\hat{I} < I_t$) [21, 29, 30]. In IS [26], $\hat{I}$ is estimated by measuring the average number of idle slots between transmission attempts, which can be expressed as

$$\hat{I} = \frac{\sum_{k=0}^{M} I_k}{M}, \tag{23}$$

where I is the number of idle slots observed between two transmission attempts and M is the maximum number of transmission attempts (note: differs from m = the estimated number of integrated ONT-APs). The refined IS algorithm in [29] sets the value of M depending on the accuracy of the estimate $\hat{I}$. If the difference between estimate $\hat{I}$ and target value I_t is within 0.75, M becomes one-quarter of the CW size or else M is reduced to five in order to speed up convergence when the estimate is clearly off target. Fig. 4 indicates that the obtained total throughput S is within 97% of the target throughput when the WUs use IS as their adaptation mechanism. Furthermore, it is also observed that when the number of BSSs increases, the DL throughput S_{ap} is ~ 8% lower than its target throughput, whereas the UL throughput S_{wu} is about 3% higher than its target throughput. Therefore, the resultant S_{wu}/S_{ap} ratio k_{mea} is nearly 8% lower than target k. Overall, the obtained results are comparable to the respective target values with a minor difference, which is not significant, most probably resulted from the effect of the AIMD algorithm as discussed in [35].

However, it is surprising to note that the fairness in channel utilisation, F, deteriorates as the number of BSSs grows dropping below 0.5 when $m \geq 12$ (Fig. 6). Jain's fairness index, F, is given by the spread in CW_{wu} over all WUs at the end of the simulation

$$F = \frac{\left(\sum_{i=0}^{n} \frac{2}{CW_{wui} + 1}\right)^2}{n \sum_{i=0}^{n} \left(\frac{2}{CW_{wui} + 1}\right)^2} \tag{24}$$

The range of F lies within 0–1, where a value closer to 1 implies better fairness [36]. The figure shows that good fairness is only possible when the network size is small ($m \leq 5$).

According to the principle of IS, all contending stations, using the IS scheme, are trying to reach the target value I_t and set their transmission probabilities to target P_{tr_t}. The relationship is given by

$$I_t = \frac{1 - P_{tr_t}}{P_{tr_t}} \tag{25}$$

Hence, from (1), the CW sizes of all WUs will ideally converge to the target value

$$CW_{wu}^{opt} = \frac{2}{\left(\frac{1 - (1 - P_{tr_t})}{\left(1 - \frac{2}{CW_{ap} + 1}\right)^m}\right)^{1/n}} - 1, \tag{26}$$

irrespective of their initial CW_{wu} states. However, this is not always the case as shown next. When the network is large (large m, large n), every WU adapts to a different value of CW as illustrated in Fig. 7. The figure shows the cdf of CW_{wu} for a network with $m = 30$ APs having fixed CW_{ap}^{opt}, and $n = 120$ WUs contending the channel using the IS scheme. At the beginning of the simulation ($t = 0$ s) every WU contends the channel with a CW size randomly chosen within the range (16, $2CW_{wu}^{opt}$). After 50 s, the CW sizes of all WUs do not show any sign that they will converge to the common value but diverge away from the initial states. Finally, as the time approaches 100 s, two classes of CW sizes are created where the first class dominates most of the channel bandwidths while the second class starves. The huge gap between the two classes of CW sizes anticipates the instability of the scheme and further deteriorating the fairness between all WUs.

Despite the fact that one class of WUs are starving and growing poor throughput, it does not deteriorate S_{wu} as it is supported by another class of WUs, which hog the channel, contributing more throughput for the UL, S_{wu}. Therefore, the resultant k_{mea} is still close to the target value and the channel utilisation remains unaffected by the instability of the IS scheme. It is worth noting that the resultant S_{ap} also remains unaffected because all the APs use a fixed CW size.

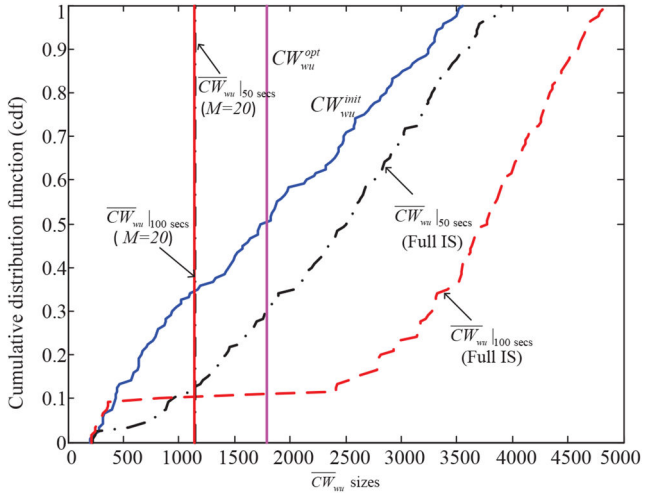

Fig. 7 *Cumulative distribution function (cdf) of* $\mathrm{CW_{wu}}$ *with 120 WUs (from 30 BSSs) contending stations*

Table 3 Performance comparison for $M = 5$, 20, and 1000

M	5	20	1000	Target
$\bar{I}$	1.70	2.34	3.17	3.26
$\overline{\mathrm{CW}}_{\mathrm{wu}}$	826	1481	1666	1791
$\sigma_{\mathrm{CW_{wu}}}$	75.56	65.39	52.2	0
S	0.43	0.438	0.442	0.454
S_{ap}	0.137	0.168	0.213	0.227
S_{wu}	0.293	0.271	0.229	0.227
$\bar{k}_{\mathrm{mea}}$	2.09	1.65	1.08	1
convergence time, s	1.42	5.79	297.51	0

while *active* **do**
  if *DATA received* **then**
    $P_u = P_u + 1$;
  end
  if *DATA transmitted* **then**
    $P = P + 1$;
    if *ACK received* **then**
      $P_d = P_d + 1$;
    end
  end
  if $P = P_{set}$ **then**
    $\Delta = (P_u - k * P_d)$;
    $\delta = \frac{\Delta}{max(k*P_d, P_u)} CW_{ap}$;
    $CW_{ap} = CW_{ap} - \varphi\delta$;
    $P = 0$;
    $P_u = 0$;
    $P_d = 0$;
    $\delta = 0$;
  end
end

Fig. 8 *Algorithm 1: APSA algorithm*

6 Synchronous updates

In a study of an *ad hoc* WLAN (i.e. with $m = 0$), Hassan *et al*. [35] concluded that the fairness problem in the IS scheme arose due to the combined effects of bias in the AIMD algorithm, non-synchronous updating of the CW, and the varying length of M among stations. As an alternative solution, one of these three factors is removed, the varying length of M is fixed to allow synchronous updates across all stations. Therefore, each station has an equal chance of updating its CW sizes and will eventually converge to the common value to achieve perfect fairness as demonstrated by the vertical line in Fig. 7 for $M = 20$.

Table 3 summarises the comparison between different values of M ($M = 5$, 20, and 1000) pertaining to their performance metrics. As expected, the accuracy of the estimate $\hat{I}$ increases with M. The mean of the estimate $\bar{I}$ ($= E(\hat{I})$) for $M = 1000$ varies within 3% of the target value, I_t, compared to 47% for $M = 5$. It is also observed that lower $\bar{I}$ estimates cause the $\mathrm{CW_{wu}}$ sizes to converge to lower than optimum values giving the WUs more chances to transmit. As a result, S_{wu} increases and deteriorates the fairness between DL and UL transmissions. Note that $\mathrm{CW_{ap}}$ remains fixed. For example, with $M = 5$ resulted in $\overline{\mathrm{CW}}_{\mathrm{wu}} = 826$ some 54% lower than target. Thus, allowing the WUs to gain higher throughput (S_{wu} =0.293, 28% higher than target) and worsen the fairness between DL and UL as indicated by the 109% increase in k_{mea} to 2.09. Moreover, the reduction in $\overline{\mathrm{CW}}_{\mathrm{wu}}$ causes increased collisions which degrade the overall throughput by 5%; somewhat less than anticipated considering the almost halving of the $\overline{\mathrm{CW}}_{\mathrm{wu}}$.

Conversely, setting $M = 1000$ improves all metrics. $\overline{\mathrm{CW}}_{\mathrm{wu}}$ converges to within 93% of the optimum target value, and the fairness between UL and DL is significantly improved (k_{mea} =1.08) to within 92% of its target value. Furthermore, the variance in $\mathrm{CW_{wu}}$ reduces as M increases, implying that the throughput fairness between WUs is also improved.

In spite of higher M giving better performance, it requires a longer time to converge. The comparison summary in Table 3 reveals that the convergence time is directly proportional to M. For example, the convergence time for $M = 1000$ is about 200 times longer than $M = 5$. Clearly, the benefits of better performance are offset by the downside of longer convergence time. Therefore, in this study, we choose $M = 20$ as a good compromise value. Although fairness, k, is much improved (cf. $M = 5$), it is still 65% away from the designed value. In the following section, we propose an alternative algorithm to improve fairness without jeopardising the convergence time.

7 AP self-adapting algorithm

This section proposes the AP self-adapting (APSA) algorithm to assist the network to achieve the desired k. This approach requires every AP in the network to monitor the measured $S_{\mathrm{wu}}/S_{\mathrm{ap}}$ ($= k_{\mathrm{mea}}$) in its respective BSS by counting the number of successfully transmitted packets, P_{d} (forming the DL throughput S_{ap}) and the received packets, P_{u} (forming the UL throughput S_{wu}). Each AP periodically adjusts its $\mathrm{CW_{ap}}$ after every P_{set} transmissions so that the observed k_{mea} will reach the desired k. The AP alters its CW size by δ, where

$$\delta = \frac{P_u - k \times P_{\mathrm{d}}}{\max\,(k \times P_{\mathrm{d}} P_{\mathrm{u}})} \mathrm{CW_{ap}}, \tag{27}$$

to equalise the discrepancy between k_{mea} and k. In order to provide a smoother behaviour of the obtained CW size, a smoothing factor φ is weighted into δ where $0 < \varphi \leq 1$. Algorithm 1 (see Fig. 8) describes APSA formally.

Next, the network performance is evaluated when the modified IS ($M = 20$) and APSA schemes are incorporated together. P_{set} is a compromise between accuracy and convergence time, similar to M in the previous section. Fig. 9 shows the cdf of $\mathrm{CW_{ap}}$ for a system of 30 APs after convergence. The variation in $\mathrm{CW_{ap}}$ is directly attributed to the accuracy of estimating k_{mea} and hence P_{set}. The simulations show 80% of APs have the variation of CWs within ± 6, ± 12 or $\pm 24\%$ of the mean value of $\bar{\mathrm{CW}}_{\mathrm{ap}} = 348$ for $P_{\mathrm{set}} = 300$, 100, and 30, respectively. A similar trend is shown for the deviation in k_{mea} after it has reached convergence (Fig. 10, table of $\sigma_{k_{\mathrm{mea}}}$). The convergence time, however, increases with P_{set} and is dominated by the time it takes to the first estimates as indicated by the waiting time before the starting transient. Once convergence starts, it is generally fast and accurate. Here, we choose $P_{\mathrm{set}} = 100$ as 10 s convergence time is too long with $P_{\mathrm{set}} = 300$ and the spread of $\pm 24\%$ in $\mathrm{CW_{ap}}$ is too large when $P_{\mathrm{set}} = 30$.

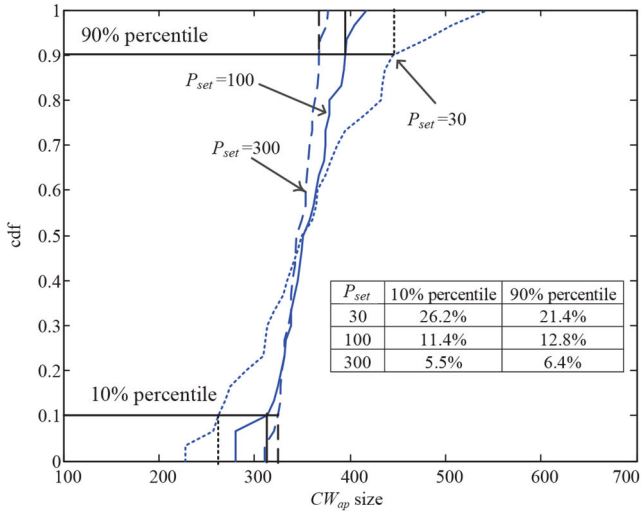

Fig. 9 *Cdf of* CW_{ap} *with 120 WUs (from 30 BSSs) contending stations for different* $P_{set} = 30, 100$ *and 300 (*$k = 1$ *and* $\varphi = 1$*)*

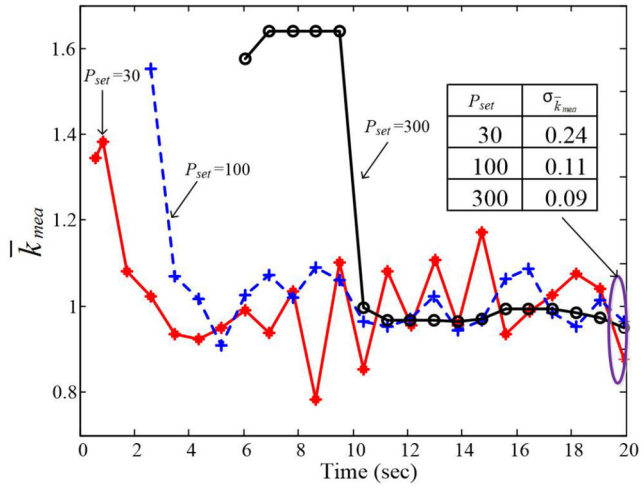

Fig. 10 *Convergence time for one AP in the network with 30 BSSs to reach the desired* $k = 1$ *for different* $P_{set} = 30,100,$ *and 300 with* $\varphi = 1$

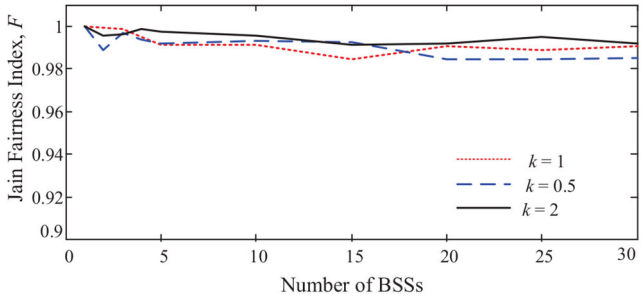

Fig. 11 *Fairness between APs for networks with k = 0.5, 1, and 2*

Fig. 4 shows that the APSA algorithm exactly balances S_{wu} and S_{ap} when $k = 1$, irrespective of network size, m. Nonetheless, the 2.6% throughput degradation (relative to the target) remains almost unchanged caused by the choice of $M = 20$ in the IS section of the algorithm. However, this reduction is marginal, more than outweighed by the benefits of achieving perfect fairness between all WUs, as demonstrated by the straight vertical line in Fig. 7.

A corollary of the APSA algorithm was that the AP's CW_{ap} size was no longer fixed, which might affect their fairness. Therefore, we measure the fairness between APs using (24) for different numbers of BSSs, with targets of $k = 0.5, 1$ and 2. Interestingly, it is apparent from the plots in Fig. 11 that the impact of APSA on the fairness between APs is minimal as the measured F is maintained above 0.98 for all network scenarios in this study. Fig.

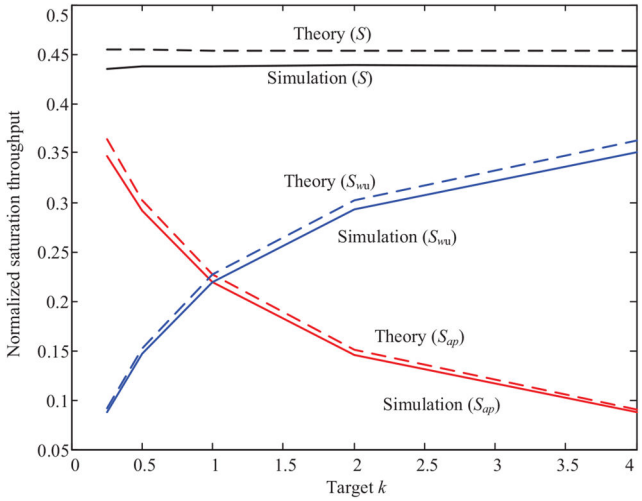

Fig. 12 *Normalised saturation throughputs (total, DL, and UL) for 30 BSSs network scenario as the network's target k varies from 0.25 to 4*

Table 4 Equilibrium throughput for five BSSs having different target k

		IS and APSA			IS, APSA and WUA		
k	n^j	S_{ap}	S_{wu}	S	S_{ap}	S_{wu}	S
1	4	0.039	0.039	0.078	0.044	0.045	0.089
1	4	0.039	0.038	0.077	0.044	0.045	0.089
0.5	4	0.078	0.039	0.117	0.059	0.029	0.088
0.5	4	0.078	0.039	0.117	0.059	0.029	0.088
2	4	0.020	0.039	0.059	0.030	0.059	0.089

12 depicts the throughput performance of 30 BSSs when target k varies from 0.25 to 4. It is evident that throughput is within 96% of the theoretical optimum, indicating k_{mea} remains close to the k. Thus, the APSA algorithm can handle a wide range of m and k.

Furthermore, we evaluate the performance of the IS+APSA scheme when five BSSs operate in the same spectrum but with different priority factors k, as specified in Table 4. By comparing the throughput columns, S_{ap} and S_{wu} (without WUA), every BSS achieves target k, corroborating the effectiveness of the APSA and IS algorithms. Every AP plays its role to maintain the k_{mea} within the set target k in its BSS while all the WUs equally share the remaining bandwidth using the IS scheme.

Therefore, each BSS gains equal UL throughput S_{wu} (column 2) irrespective of target k. However, the DL throughput S_{ap} is inversely proportional to target k (i.e. the higher k, the lower the DL throughput S_{ap}), validating the impact of the APSA algorithm. For instance, for the case $k = 0.5$, the AP keeps on reducing its CW size in order to ensure the DL throughput (S_{ap}) is twice the UL throughput (S_{wu}), while for $k = 2$, it keeps on increasing its CW size to ensure S_{ap} is half of the S_{wu}. This unbalance behaviour affects the throughput fairness amongst BSSs as demonstrated in Table 4 (column 3). The two BSSs with $k = 0.5$ dominate 52% of the total throughput leaving two BSSs with $k = 1$ and one BSS with $k = 2$ to obtain 35 and 13% of the total throughput, respectively. The following section suggests a technique to equalise the fairness amongst BSSs.

8 WUA algorithm

The WUA algorithm introduces a mechanism to ensure the chance of a WU to transmit is dependent on target k set in its respective BSS so that the total throughput per BSS across the network is fairly equalised. Consider a network, which comprises m BSSs. Each BSS^j ($j = 1, 2, 3 \ldots m$) has one AP^j with n^j number of WUs and it independently sets target k^j. Every jth BSS has a probability of p_s^j of a successful transmission in either DL or UL directions, given from (6) as

$$p_s^j = \left(1 + \frac{1}{k_j}\right) p_{swu}^j \tag{28}$$

where p_{swu}^j is the probability that any one of the n^j WUs successfully transmits a packet without incurring any collision

$$p_{swu}^j = n^j p_{wu}^j (1 - p_c)\,. \tag{29}$$

Note that p_c is the probability of a collision, which is assumed constant across the network, because all the contending stations use the same transmission rate and packet size. Moreover, p_{wu}^j is the probability of WUs from BSS^j transmitting after contending the channel with the CW size of CW_{wu}^j

$$p_s^j = \left(1 + \frac{1}{k_j}\right) n^j p_{wu}^j (1 - p_c)\,. \tag{30}$$

By the principle of IS, all WUs have an equal chance of transmission (i.e. $p_{wu}^{j-1} = p_{wu}^j = p_{wu}^{j+1}$), causing p_s^j (30) to vary with k_j and n^j, the number of WUs per BSS^j. Thus, to give throughput fairness amongst BSSs, p_s^j must be scaled to remove the dependence on these two parameters. It is chosen

$$p_s^* = p_s^j \frac{2}{n^j\left(1 + \frac{1}{k_j}\right)} \tag{31}$$

such that when $k = 1$ and $n^j = 1$ there is no scaling. To achieve this, p_{wu}^j in (30) is altered at the WU to

$$p_{wu}^{j*} = \frac{2p_{wu}^j}{n^j\left(1 + \frac{1}{k_j}\right)} \tag{32}$$

by scaling the CW. Substituting (3) into (32) and assuming $\mathrm{CW} \gg 1$

$$\mathrm{CW}_{wu}^{j*} = \mathrm{CW}_{wu}^j \frac{n^j\left(1 + \frac{1}{k^j}\right)}{2}\,. \tag{33}$$

In summary, the above analysis suggests that every WU scales its current CW_{wu} (after being updated by IS) with a factor of $(n^j(1 + \frac{1}{k})/2)$ before contending the channel. The WU only needs to know local information pertaining to its BSS's n^j and k^j. The former is available by monitoring the traffic from the AP and identifying its address fields and the latter must be periodically broadcast from the AP^j.

The simulation scenario described in Table 4 is repeated using the WUA algorithm. The UL throughput S_{wu} in each BSS varies with the set priority target k^j, and n^j such that every BSS is forced to have an equal throughput, S (column 6) irrespective of k^j. Note the measured k_{mea} remains close to the target value, k^j.

The previous simulations assumed the number of users per BSS is fixed at $n^j = 4$. Table 5 shows results for variable n^j per BSS. There are still $m = 5$ APs and $n = 20$ WUs, but the WUs are no longer evenly spread between the BSSs. In all cases, the APSA algorithm maintains the measured $k_{mea} = S_{wu}/S_{ap}$ close to the target, while the IS algorithm remains constant throughput per WU. The total throughput S per BSS (column 3) is now dependant on both n^j and k. The fairness is restored between BSSs when the WUA algorithm is included. Also, note the total throughput, S, is independent of n^j, which means the more WUs, the less throughput each gets.

Finally, the robustness of the network is evaluated when all $m = 30$ APs and $n = 120$ WUs in the combined IS, APSA, and WUA schemes. The plot in Fig. 13 demonstrates the convergence

Table 5 Equilibrium throughput for five BSSs having different target k and n^j

			IS and APSA			IS, APSA, and WUA		
j	k	n^j	S_{ap}	S_{wu}	S	S_{ap}	S_{wu}	S
1	1	2	0.020	0.020	0.040	0.046	0.045	0.091
2	1	6	0.059	0.057	0.116	0.045	0.043	0.088
3	0.5	2	0.039	0.019	0.058	0.060	0.029	0.089
4	0.5	6	0.119	0.057	0.176	0.060	0.029	0.089
5	2	4	0.020	0.038	0.058	0.030	0.059	0.089

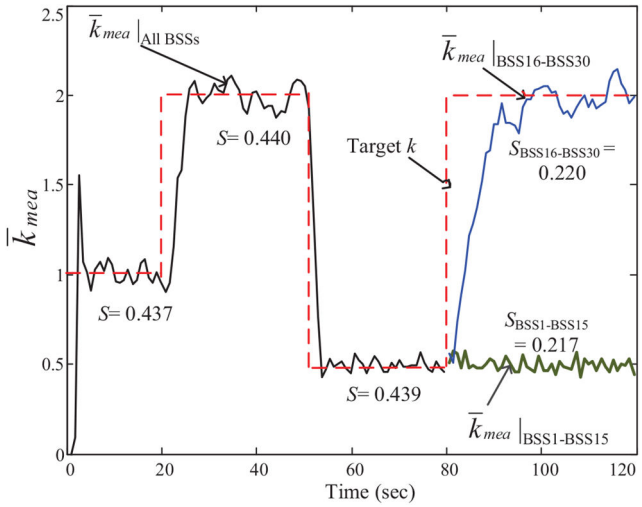

Fig. 13 *Network (30 BSSs) responses to the changes of target k ($\varphi = 1$)*

behaviour of $\bar{k}_{mea}$ when target k changes across the network. It is evident that the proposed scheme quickly responds to the changes in k: 5 s are required for the network to change from $k = 1$ to $k = 2$ and a similar time to change from $k = 2$ to $k = 0.5$. However, a somewhat longer 12 s is required for 15 BSSs to reach $k_{mea} = 2$ (from $k_{mea} = 0.5$) while the other 15 BSSs remain at their $k = 0.5$ setting. At this state, despite k difference, both classes of BSSs have almost equal throughputs, with the difference being < 1.5% as indicated by S_{BSS} values in Fig. 13.

9 Conclusions

This study proposed a series of schemes to improve the performance of the WLAN in multiple BSSs scenario, which resembles the wireless side of the FiWi networks. The performance of the wireless component is optimised by taking advantage of the common fibre connection going to all the integrated ONT–APs and the broadcast nature of the GPON downstream transmission from which m number of active ONT–AP can be estimated. The estimate m is then used in our proposed scheme to compute the optimum CW_{ap} size (12)–(14). Alternatively, the CW_{ap} values can be pre-calculated and stored in a look-up table. The study analytically extends the AAP scheme into the multiple BSSs scenario. Priority is given to the APs by using constant CW sizes (analytically derived) while the WUs equally share the remaining bandwidth using the IS adaptation method. The study revealed two classes of users, those that dominate transmissions and those that starve. Instability arises when bias from the AIMD convergence process interacts with the adaptive idle slot-sensing mechanism. Therefore, the IS scheme is simplified by forcing all WUs to a fixed IS sensing period. As a result, the fairness between WUs is improved but UL/ DL fairness, k_{mea}, remains a problem. Thus, every AP periodically adjusts its CW_{ap} to reach the desired UL/DL throughput target, k. However, the IS+APSA algorithm generates unfairness between BSSs with different k targets. The WUA algorithm recuperates the fairness between BSSs by scaling the current CW_{wu} based on the required k^j and the number of BSS users. The network achieves the desired fairness between UL and

DL as well as between BSSs while maintaining the difference of throughputs within 4% of theoretical optimum. The network responds to changes in k within a maximum of 12 s. In conclusion, the combined IS+APSA+WUA scheme is well fitted for the wireless side (WLAN networks with multiple BSSs sharing the same frequency channel) of the FiWi networks. Each station in the BSS is given a fair transmission opportunity to fully utilise the huge bandwidth capacity provided by the GPON (backhaul). Further work is required to evaluate the accuracy of the estimate m obtained from the GPON and consequently analyse the backend effect of FiWi networks on our proposed algorithms.

10 Acknowledgments

The authors would like to thank the Ministry of Education Malaysia, Universiti Malaysia Terengganu and the administration of Universiti Teknologi Malaysia for the financial assistance through Professional Development Research University and Fundamental Research Grant Scheme fund with vote numbers 04E58 and 4F961, respectively.

11 References

[1] Bhatt, U.R., Chhabra, A., Upadhyay, R.: 'Fiber-wireless (Fi-Wi) architectural technologies: a survey'. Int. Conf. on Electrical, Electronics, and Optimization Techniques (ICEEOT), Chennai, India, 2016, pp. 519–524

[2] Liu, J., Guo, H., Nishiyama, H., *et al.*: 'New perspectives on future smart FiWi networks: scalability, reliability, and energy efficiency', *IEEE Commun. Surv. Tutor.*, 2016, **18**, (2), pp. 1045–1072

[3] Ghazisaidi, N., Maier, M.: 'Fiber-wireless (FiWi) access networks: challenges and opportunities', *IEEE Netw.*, 2011, **25**, (1), pp. 36–42

[4] Aurzada, F., Lévesque, M., Maier, M., *et al.*: 'FiWi access networks based on next-generation PON and gigabit-class WLAN technologies: a capacity and delay analysis', *IEEE/ACM Trans. Netw.*, 2014, **22**, (4), pp. 1176–1189

[5] Maier, M.: 'FiWi access networks: future research challenges and moonshot perspectives'. 2014 IEEE Int. Conf. on. Communications Workshops (ICC), Sydney, Australia, 2014, pp. 371–375

[6] Shen, G., Tucker, R.S., Chae, C.J.: 'Fixed mobile convergence architectures for broadband access: integration of EPON and WiMAX [topics in optical communications]', *IEEE Commun. Mag.*, 2007, **45**, (8), pp. 44–50

[7] Grzybowski, L., Hasbi, M., Liang, J.: 'Transition from copper to fiber broadband: the role of connection speed and switching costs', *Inf. Econ. Policy*, 2018, **42**, pp. 1–10

[8] Bladocha, A.: 'New market panorama data at the FTTH conference 2018'. PR Market Panorama', 2018. Available at http://www.fibre-systems.com/news/ftth-conference-2018/-europe-sees-20-growth-fibre-subscribers

[9] Ranaweera, C.S., Iannone, P.P., Oikonomou, K.N., *et al.*: 'Design of cost-optimal passive optical networks for small cell backhaul using installed fibers', *IEEE/OSA J. Opt. Commun. Netw.*, 2013, **5**, (10), pp. A230–A239

[10] Liu, Y., Guo, L., Wei, X.: 'Optimizing backup optical-network-units selection and backup fibers deployment in survivable hybrid wireless-optical broadband access networks', *J. Lightwave Technol.*, 2012, **30**, (10), pp. 1509–1523

[11] Guo, L., Liu, Y., Wang, F., *et al.*: 'Cluster-based protection for survivable fiber-wireless access networks', *J. Opt. Commun. Netw.*, 2013, **5**, (11), pp. 1178–1194

[12] Yu, Y., Ranaweera, C., Lim, C., *et al.*: 'Optimization and deployment of survivable fiber-wireless (FiWi) access networks with integrated small cell and WiFi'. 2015 IEEE Int. Conf. on Ubiquitous Wireless Broadband (ICUWB), Montreal, Canada, 2015, pp. 1–5

[13] Hassan, W.H.W., King, H., Ahmed, S., *et al.*: 'Transmission priority scheme with adaptive backoff technique in fiber-wireless networks', *EURASIP J. Wirel. Commun. Netw.*, 2015, **2015**, (1), pp. 99

[14] Kim, J.Y., Kim, S.H., Sung, D.K.: 'Hybrid ARQ-based fairness enhancement in uplink WLAN', *IEEE Trans. Wirel. Commun.*, 2018, **17**, (7), pp. 4362–4373

[15] Katayama, Y., Umehara, D., Wakasugi, K.: 'A mathematical model of access control to allocate downlink bandwidth in high-density wireless LAN'. 2017 11th Int. Conf. on Signal Processing and Communication Systems (ICSPCS), Gold Coast, Australia, 2017, pp. 1–7

[16] Ando, R., Hamamoto, R., Obata, H., *et al.*: 'A priority control method for media access control method SP-MAC to improve throughput of bidirectional flows', *IEICE Trans. Inf. Syst.*, 2017, **100**, (5), pp. 984–993

[17] Umehara, D., Murata, H., Denno, S.: 'IEEE 802.11 DCF with successful transmission priority'. 2015 9th Int. Conf. on Signal Processing and Communication Systems (ICSPCS), Cairns, Australia, 2015, pp. 1–7

[18] Gao, Y., Dai, L.: 'Optimal downlink/uplink throughput allocation for IEEE 802.11 DCF networks', *IEEE Wirel. Commun. Lett.*, 2013, **2**, (6), pp. 627–630

[19] Wang, C.: 'Achieving per-flow and weighted fairness for uplink and downlink in IEEE 802.11 WLANs', *EURASIP J. Wirel. Commun. Netw.*, 2012, **2012**, (1), pp. 239

[20] Abeysekera, B.H.S., Matsuda, T., Takine, T.: 'Dynamic contention window control mechanism to achieve fairness between uplink and downlink flows in IEEE 802.11 wireless LANs', *IEEE Trans. Wirel. Commun.*, 2008, **7**, (9), 3517–3525

[21] Lopez-Aguilera, E., Heusse, M., Grunenberger, Y., *et al.*: 'An asymmetric access point for solving the unfairness problem in WLANs', *IEEE Trans. Mob. Comput.*, 2008, **7**, (10), pp. 1213

[22] Kim, S.W., Kim, B.S., Fang, Y.: 'Downlink and uplink resource allocation in IEEE 802.11 wireless LANs', *IEEE Trans. Veh. Technol.*, 2005, **54**, (1), pp. 320–327

[23] Micó, F., Villalón, J., Valverde, A., *et al.*: 'Guaranteed access mode for downlink traffic over IEEE 802.11 WLANs'. 2011 4th Joint IFIP Wireless and Mobile Networking Conf. (WMNC), Toulouse, France, 2011, pp. 1–7

[24] Lim, W.S., Kim, D.W., Suh, Y.J.: 'Achieving fairness between uplink and downlink flows in error-prone WLANs', *IEEE Commun. Lett.*, 2011, **15**, (8), pp. 822–824

[25] Min, G., Hu, J., Woodward, M.E.: 'Modeling and analysis of TXOP differentiation in infrastructure-based WLANs', *Comput. Netw.*, 2011, **55**, (11), pp. 2545–2557

[26] Heusse, M., Rousseau, F., Guillier, R., *et al.*: 'Idle sense: an optimal access method for high throughput and fairness in rate diverse wireless LANs', ACM SIGCOMM Computer Communication Review (ACM), Philadelphia, PA, USA, 2005, vol. 35 (4)

[27] Hong, K., Lee, S., Kim, K., *et al.*: 'Channel condition based contention window adaptation in IEEE 802.11 WLANs', *IEEE Trans. Commun.*, 2012, **60**, (2), pp. 469–478

[28] Le, Y., Ma, L., Cheng, W., *et al.*: 'A time fairness-based MAC algorithm for throughput maximization in 802.11 networks', *IEEE Trans. Comput.*, 2015, **64**, (1), pp. 19–31

[29] Grunenberger, Y., Heusse, M., Rousseau, F., *et al.*: 'Experience with an implementation of the idle sense wireless access method'. Proc. 2007 ACM CoNEXT Conf. (ACM), New York, NY, USA, 2007, pp. 24

[30] Nassiri, M., Heusse, M., Duda, A.: 'A novel access method for supporting absolute and proportional priorities in 802.11 WLANs'. INFOCOM 2008. The 27th Conf. on Computer Communications. IEEE, Phoenix, AZ, USA, 2008, pp. 709–717

[31] ITU.T Recommendation, G.984.3: 'Gigabit-capable passive optical networks (GPON): transmission convergence layer specification', ITU-T Study Group, 2008

[32] Hassan, W.H.W., King, H., Faulkner, M.: 'Modified backoff technique in fiber-wireless networks'. 2012 IEEE 23rd Int. Symp. on Personal Indoor and Mobile Radio Communications (PIMRC), Sydney, Australia, 2012, pp. 431–435

[33] Bianchi, G.: 'Performance analysis of the IEEE 802.11 distributed coordination function', *IEEE J. Sel. Areas Commun.*, 2000, **18**, (3), pp. 535–547

[34] IEEE Computer Society LAN MAN Standards Committee and others: 'Wireless LAN medium access control (MAC) and physical layer (PHY) specifications', ANSI/IEEE Std 80211-1999, 1999

[35] Hassan, W.H.W., King, H., Ahmed, S., *et al.*: 'WLAN fairness with idle sense', *IEEE Commun. Lett.*, 2015, **19**, (10), pp. 1794–1797

[36] Jain, R.K., Chiu, D.M.W., Hawe, W.R.: '*A quantitative measure of fairness and discrimination*' (Eastern Research Laboratory, Digital Equipment Corporation, Hudson, MA, 1984)

12 Appendix

12.1 Full derivation of saturation throughput S

Considering the fact that the contention of a radio channel can evolve between three states: idle 'i', collision 'c', and successful transmission 's', which gives

$$p_{\mathrm{i}} + p_{\mathrm{c}} + p_{\mathrm{s}} = 1. \tag{34}$$

By definition, normalised saturation throughput S is expressed as the fraction of time the channel is used to successfully transmit payload bits

$$S = \frac{p_{\mathrm{s}} T_{\mathrm{payload}}}{p_{\mathrm{i}} T_{\mathrm{i}} + p_{\mathrm{c}} T_{\mathrm{c}} + p_{\mathrm{s}} T_{\mathrm{s}}}. \tag{35}$$

Note that collision and successful transmission states give the impression that the channel is busy indicating that there is at least one transmission on the channel. Hence, the transmission probability P_{tr} is

$$P_{\mathrm{tr}} = p_{\mathrm{c}} + p_{\mathrm{s}}, \tag{36}$$

which further yields

$$P_{\mathrm{c}} + P_{\mathrm{s}} = 1, \tag{37}$$

where

$$P_{\mathrm{c}} = \frac{p_{\mathrm{c}}}{P_{\mathrm{tr}}} \tag{38}$$

and

$$P_{\mathrm{s}} = \frac{p_{\mathrm{s}}}{P_{\mathrm{tr}}}. \tag{39}$$

Corroborating (34) and (36) gives

$$p_{\mathrm{i}} = 1 - P_{\mathrm{tr}}. \tag{40}$$

Finally, using (35), (38)–(40), the normalised saturation throughput S is derived

$$S = \frac{P_{\mathrm{s}} P_{\mathrm{tr}} T_{\mathrm{payload}}}{(1 - P_{\mathrm{tr}}) T_{\mathrm{i}} + P_{\mathrm{s}} P_{\mathrm{tr}} T_{\mathrm{s}} + (1 - P_{\mathrm{s}}) P_{\mathrm{tr}} T_{\mathrm{c}}}.$$